JACS
JOURNAL OF THE AMERICAN CHEMICAL SOCIETY
Article
pubs.acs.org/JACS

Chiroptical Inversion in Helical Si–Si Bond Polymer Aggregates

Nozomu Suzuki,[†] Michiya Fujiki,*[,†] Ruth Kimpinde-Kalunga,[‡] and Julian R. Koe*[,‡]

[†]Graduate School of Materials Science, Nara Institute of Science and Technology, 8916-5 Takayama, Ikoma, Nara, 630-0192, Japan
[‡]Department of Material Science, International Christian University, 3-10-2 Osawa, Mitaka, Tokyo, 181-8585, Japan

Supporting Information

ABSTRACT: To elucidate the factors involved in the chiroptical properties of polymer aggregates composed of helical building blocks, a series of rigid rod helical poly[alkyl-(*S*)-2-methylbutylsilane]s (achiral alkyl side chains = ethyl, *n*-propyl, *n*-butyl, *n*-pentyl, *n*-hexyl) have been investigated. It was found that the chiroptical sign in the circular dichroism (CD) spectra of the polysilane aggregates depends on the achiral side chain length and cosolvent fraction. Concerning the achiral side chains, the *n*-propyl group was of a critical length for solvent-dependent chiroptical inversion on aggregation. This unique side chain length-dependent chiroptical inversion was theoretically predictable by using the novel approach of combining the cholesteric hard-core model and exciton chirality method. The latter was also investigated theoretically by Gaussian 03 (TD-DFT, B3LYP, 6-31G(d) basis set) calculations applied to two spatially arranged helical Si–Si bonded decamer models.

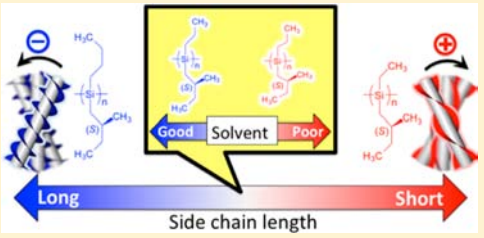

1. INTRODUCTION

The helix is one of the most striking examples of chiral structures and is seen not only in biomolecules[1,2] but also in synthetic macromolecules[3−9] and supramolecules.[10−18] To control the intra- and interhelical structure of the molecules, key geometric parameters such as the molecular size, topology, stereochemistry, and shape are critical.[4] Further, using simple chiral π- and σ-conjugating helical polymers[19−27] permits the application of their chiroptical properties in optical devices such as sensors, switches, and memory toward chemical and physical stimuli.[28−37] However, there are several obstacles to the study of the optical properties of the film states essential for device application: (1) anisotropy of the film state may result in variable chiroptical properties; (2) different crystalline phases[38,39] coexist in the film states which complicate the optical properties; and (3) most conjugating helical polymers have multiple chromophores and/or show vibronic sidebands which complicate the UV and circular dichroism (CD) spectra. One way to circumvent problems 1 and 2 is to study samples in aggregate states in which intermolecular interactions occur as in film states, but problems due to anisotropy and crystallinity do not arise. Use of an ideal conjugated polymer with a single chromophore and no vibronic sideband solves problem 3.

Among optical properties including the sergeant-soldier and majority-rule type chiroptical amplifications,[35,37] chiroptical inversion is a particularly intriguing phenomenon. In most cases, however, the relationship between the higher order structure and the chiroptical characteristics is not fully understood due to the lack of theoretical background. Several factors governing higher order chiral structures have been proposed by a number of workers. For instance, the rigidity and twisting ability of the main chain helix,[28] the geometry of the individual helical building blocks,[29] alternation in $\pi-\pi$ stacking motif,[30−32] and subtle balance between repulsive and attractive chiral interactions[33] have been discussed.

In a previous paper, we described chiroptical inversion in the aggregates of a series of polysilanes with a mesogenic aryl side chain and a chiral (*S*)-2-methylbutyl side chain, concluding that the different inversion characteristics arose due to the difference in helical diameter of the individual polymer chains.[29] However, the relationship between the higher order structure and chiroptical property was complicated because the aryl–alkyl polysilanes contain two chromophoric transitions in the UV region: Siσ–Siσ* and Arπ–Arπ*.[40,41]

In the present work, we designed a series of optically active dialkylpolysilanes bearing chiral (*S*)-2-methylbutyl and achiral alkyl side chains (**1**−**5**, Chart 1) and extended the theoretical model to study the higher order structures of helical polymers. These helical dialkylpolysilanes feature a unique Siσ-Siσ* transition around 300 nm without vibronic sidebands in the UV and CD spectra. In addition, when these polymers form aggregates, there are no $\pi-\pi$ interactions, which enabled us to focus just on the helical geometry and the solvation effects. Concerning theory, we combined the cholesteric hard-core model[29,42−44] and exciton chirality method,[45−48] which permitted discussion not only of the inversion but also of the aggregate CD signal sign. The use of these ideal polymers and our pioneering extension of theory should clarify the relationship between the higher order structure and chiroptical properties in aggregate and film states.

Received: June 4, 2013
Published: August 6, 2013

   dx.doi.org/10.1021/ja405570q | J. Am. Chem. Soc. 2013, 135, 13073−13079

Chart 1. Chemical Structures of Poly[alkyl-(*S*)-2-methylbutylsilane]s with Different Achiral Alkyl Chains: Ethyl (1), *n*-Propyl (2), *n*-Butyl (3), *n*-Pentyl (4), and *n*-Hexyl (5)

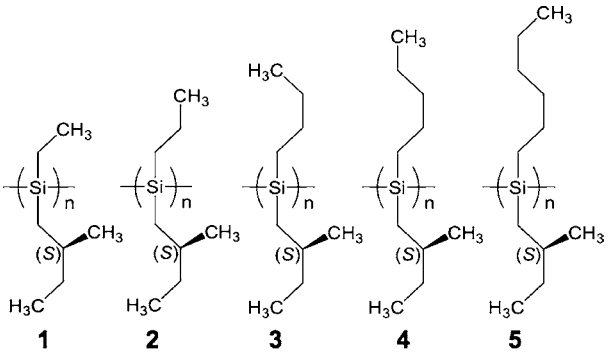

2. RESULTS AND DISCUSSION

All polysilanes (**1**−**5**) dissolved homogeneously in dilute toluene (a good solvent) typically showed intense narrow UV and positive-signed CD bands around 310 nm (Kuhn's anisotropy, g_{CD} (= $\Delta\varepsilon/\varepsilon$) = 1.95−2.28 × 10^{-4}) due to the Siσ−Siσ* transition (Table 1 and Figure S10). The g_{CD} values suggest that **1**−**5** adopt *P*-7_3 helical structures.[49−51]

Table 1. Observed Cotton Effect Signs of Polysilanes (1−5)

polysilane	sign of the Cotton effect	
	solution (toluene)	aggregate[a] (toluene/methanol)
poly[ethyl-(*S*)-2-methylbutylsilane] (**1**)	(+)-single sign	(+)-bisign
poly[*n*-propyl-(*S*)-2-methylbutylsilane] (**2**)	(+)-single sign	(+) or (−)-bisign
poly[*n*-butyl-(*S*)-2-methylbutylsilane] (**3**)	(+)-single sign	(−)-bisign
poly[*n*-pentyl-(*S*)-2-methylbutylsilane] (**4**)	(+)-single sign	(−)-bisign
poly[*n*-hexyl-(*S*)-2-methylbutylsilane] (**5**)	(+)-single sign	(−)-bisign

[a]The signs of bisigned signals are described as from the longer wavelength side, hence (+)-bisign refers to a bisigned Cotton effect as positive at the longer wavelength extremum and negative at shorter.

Upon slow addition of methanol (a poor solvent) to dilute solutions of polymers **1**−**5**, the corresponding aggregates formed immediately. All UV λ_{max} values of these aggregates were typically blue-shifted by ca. 10 nm (Figure 1, Figures S11−15), compared to those in the homogeneous solution state and their CD spectra showed bisigned Cotton effects (Figure 1) due to exciton coupling between interacting main chains. As shown in Figure 1, **1** in a methanol/toluene solution with volume ratio (here after ratio) = 0.1/0.9 had a positive bisignate Cotton effect (signs are described referring to the longer wavelength of the two extrema) and **3** in a solution of ratio 0.4/0.6 had a negative bisignate Cotton effect.

The blue shift in the UV spectra is considered to arise due to two factors: a decrease in the Si−Si−Si−Si dihedral angle[51−54] and/or *J*- and *H*-aggregation, as proposed by Kasha.[55,56]

First, if the Si−Si−Si−Si dihedral angle diminishes from θ = 154° (*P*-7_3 helix), it reduces σ-conjugation in the Si main chain, which thus induces the blue shift. Placing the polymer in a poor solvent could lead to such a decrease in dihedral angle, since

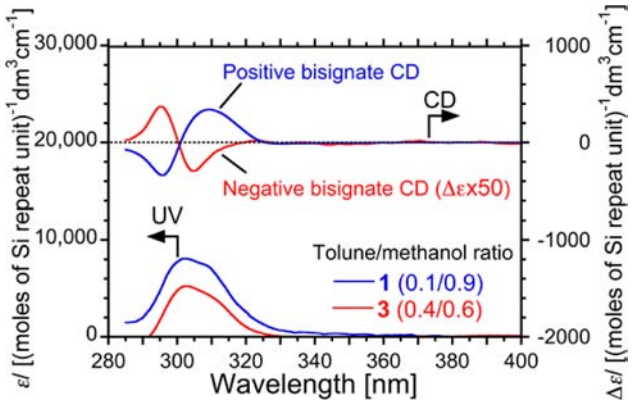

Figure 1. Comparison of UV and inverted CD spectra of **1** and **3** aggregates at 20 °C. For clarity, CD intensity of **3** was multiplied by 50.

the polymer should prefer a shorter pitch form (θ < 154°) rather than the more extended form (θ = 154°), thus reducing the surface area between solute and (poor) solvent.

Second, the blue shift could also be induced by the parallel orientation of transition dipole moments in the aggregate state, known as *H*-aggregation in the molecular exciton theory proposed by Kasha.[55,56] In this theory, two different possible arrangements of two transition dipoles were posited, one with a parallel arrangement (*H*-aggregate) giving rise to a blue shift and the other with a collinear arrangement (*J*-aggregate) giving rise to a red shift. Since *J*-aggregates are less likely to be formed than *H*-aggregates when considering the solvophobic effect of reducing the surface area between solute (polymers) and solution (toluene and methanol), the blue-shifting *H*-aggregate mode is reasonable.[57]

To discuss the reason for the blue shift, a filtration experiment[29] (5.0, 0.65, 0.22, and 0.10 μm poly(vinylidene fluoride) (PVDF) membrane filter) was carried out for **3** in toluene/methanol cosolvent (ratio = 0.5/0.5) (Figure 2). If the

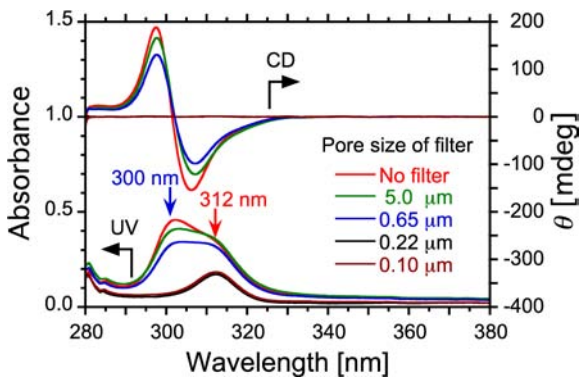

Figure 2. Result of the filtration experiment of **3** in toluene/methanol cosolvent (ratio = 0.5/0.5).

decrease in helical pitch is due to solvophobism, then there should be a decrease in pitch in both solution state and aggregate state polymer and consequently a blue-shifted λ_{max} around 300 nm. However, when the sample was filtered through the 0.1 μm PVDF membrane filter, the expected blue shift in λ_{max} to around 300 nm was not observed. This means that the blue shift cannot solely be explained as a solvophobic effect and is rather a result of the aggregation itself. The shift

dx.doi.org/10.1021/ja405570q | J. Am. Chem. Soc. 2013, 135, 13073−13079

should therefore be termed *aggregachromism* rather than *solvatochromism*.

Comparing CD data among the polymers, a unique side chain length-dependent chiroptical inversion effect was found. Among **1**−**5**, polymer **1** with the shortest achiral side chain showed a positive bisignate signal (Figure S11). In contrast, **3**−**5**, with longer achiral side chains, showed negative bisignate Cotton effects (Figures 1 and S13− S15). Polysilanes **1** and **3**−**5** maintained their chiroptical profiles regardless of the solvent ratio.

However, uniquely for **2** with an *n*-propyl group, a cosolvent ratio-dependent chiroptical inversion effect was found. When the toluene ratio in the cosolvent was relatively high (0.7/0.3 to 0.5/0.5), the aggregate showed a negative bisignate Cotton effect; conversely, when the toluene ratio was lower (0.3/0.7 to 0.1/0.9), the profiles switched to the opposite (positive) sense (Figure 3). The CD sign(s) in both solutions are summarized in Table 1.

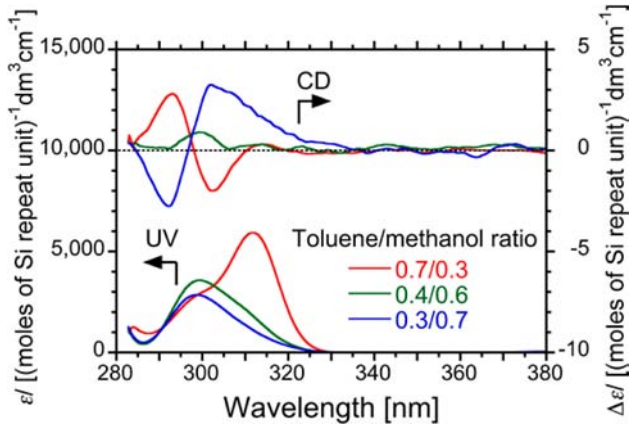

Figure 3. Comparison of CD and UV spectra of **2** aggregates at three volume ratios of toluene/methanol cosolvents.

To explain these unusual chiroptical inversion phenomena, we constructed a theoretical model by combining the cholesteric hard-core model of Straley[29,42−44] and the exciton chirality method developed by Nakanishi.[45−48] The former refers to a correlation between the chirality of individual polymer molecule helices and the chirality of the most favorable higher order skew, based on the two helical variables, pitch (p) and diameter (d). The latter predicts the sign of a CD spectrum due to coupled oscillators between two interacting chiral chromophores.

According to the cholesteric hard-core model,[44] an individual helical polymer is characterized by the helical angle Φ defined by p and d (Figure 4a). The value of p is defined as the minimum longitudinal distance between the start and end points of one full helical turn, and d is the diameter of the helix. The chiral skew of the higher order chiral structure is governed by the p/d ratio of the helix: for $p/d < \pi$ ($45° > \Phi > 0°$), a left-handed helix forms a left-handed skewed structure, while for $p/d > \pi$ ($90° > \Phi > 45°$), a left-handed helix leads to a right-handed skew, and vice versa.[44]

Using a left-handed helix as an example, d, p, Φ, "wing", and "shaft" are defined in Figure 4a, where the individual helix is depicted in a simple two-dimensional (2D) model based on the cholesteric hard-core theory. The front-facing wings are represented by diagonal lines from the upper left to the lower right (blue lines on the helix in Figure 4b), while the back-facing wings of the helix are represented by diagonal lines from upper right to lower left (red lines on the helix in Figure 4b). When one helical polymer is put in contact with another, i.e., one on top of the other with colinear transverse axes, as in Figure 4c, the contacting surfaces adopt a chiral skew with angle γ (=2Φ), such that the front-facing wings of the lower helix and back-facing wings of the upper helix become parallel, with the wings aligning with the helical grooves. The relationship between p/d ratio, γ, and Φ in degrees is given in eq 1.

$$\gamma = 2\Phi = \frac{360}{\pi} \arctan\left(\frac{p}{\pi d}\right) [\text{deg}] \quad (1)$$

Complementary to this, the exciton chirality method can semiempirically predict the signs of the split-type Cotton effect if the relative geometry of the two interacting electric transition dipole moments (here after transition dipole moment) can be determined. The sign of the exciton chirality is derived as follows: *upon looking through the centers of the two dipoles, a negative sign is defined when an anticlockwise rotation by an acute angle brings the dipole in the front onto that in the back.*[48] Since the magnitude of the aggregate transition dipole−transition dipole coupling is usually much greater than the inherent CD signal of an individual helical polymer molecule, the exciton couplet is assumed to dominate the CD of the higher order chiral structure. For dialkylpolysilanes, the lowest Siσ−Siσ* transition moment is known to be parallel to the main chain axis experimentally and theoretically.[24]

Assuming that the helical pitch, p, is constant, the combination of the cholesteric hard-core model and exciton chirality method predicts that interaction between left-handed helices of sufficiently large d (such that $p/d < \pi$) leads to a negative bisignate profile (Figure 4d). Conversely, interaction of left-handed helices of sufficiently small d (such that $p/d > \pi$) should result in a positive bisignate CD profile.

To apply the combined model to the polymers used in our experiment, it is necessary to know the handedness of the individual chains. *P*- and *M*-helical senses in dialkylpolysilanes are defined solely by the Si−Si−Si−Si dihedral angle θ: a *P*-helix results for $0° < \theta < 180°$ and an *M*-helix results for $180° < \theta < 360°$.[25] However, this does not mean that the *P*- and *M*-helical senses appear as right- and left-handed helices, respectively. Actually, a *P*-7_3 helix ($\theta \approx 154°$) is predicted by Gaussian 03 calculations (see below and Figure S16) to form a left-handed helix.[58]

The optimized 12-mer oligomers of **1**−**5** were obtained by 12-mer PM3 and p/d ratios were measured (Table S2). Though the p/d of **1** and **2** were almost the same, the calculation supported the tendency of p/d value becomes **1** > **3** > **4** > **5**. The critical value, however, was not π and it was between 1.96−1.91.[59]

In the cases of **3**−**5**, their side chains are sufficiently long and have a large d (=14.8−18.6 Å) to induce negative bisignate Cotton effects, while for **1**, with a short side chain and small d (=14.4 Å), a positive bisignate Cotton effect is evident. Thus the dependence of the sign of the Cotton effect on the p/d ratio agrees well with the experimental results.

The 2D-model *does* consider the chiral steric hindrance between front-facing and back-facing wings but *does not* consider either solvophobic effects or aggregates of more than two molecules. When two rod-like polymer molecules are induced to aggregate by the solvophobic effect of addition of a poor solvent, it is likely that the main chains form a parallel arrangement to reduce the surface area of the polymers in

dx.doi.org/10.1021/ja405570q | J. Am. Chem. Soc. 2013, 135, 13073−13079

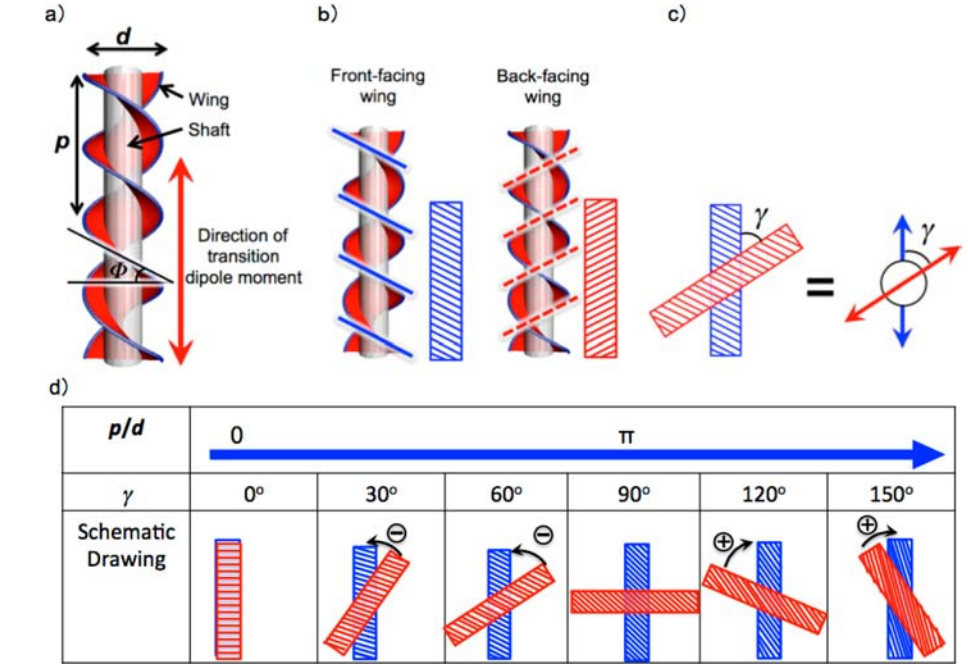

Figure 4. Schematic drawing of two-dimensional cholesteric hard-core model, exciton chirality method, and their combination. (a) Ideal left-handed helix defining *p*, *d*, Φ, "wing", "shaft", and direction of electric transition dipole moment. (b) Depiction of two-dimensional cholesteric hard-core model. (c) Relationship between the cholesteric hard-core model and expected CD sign.

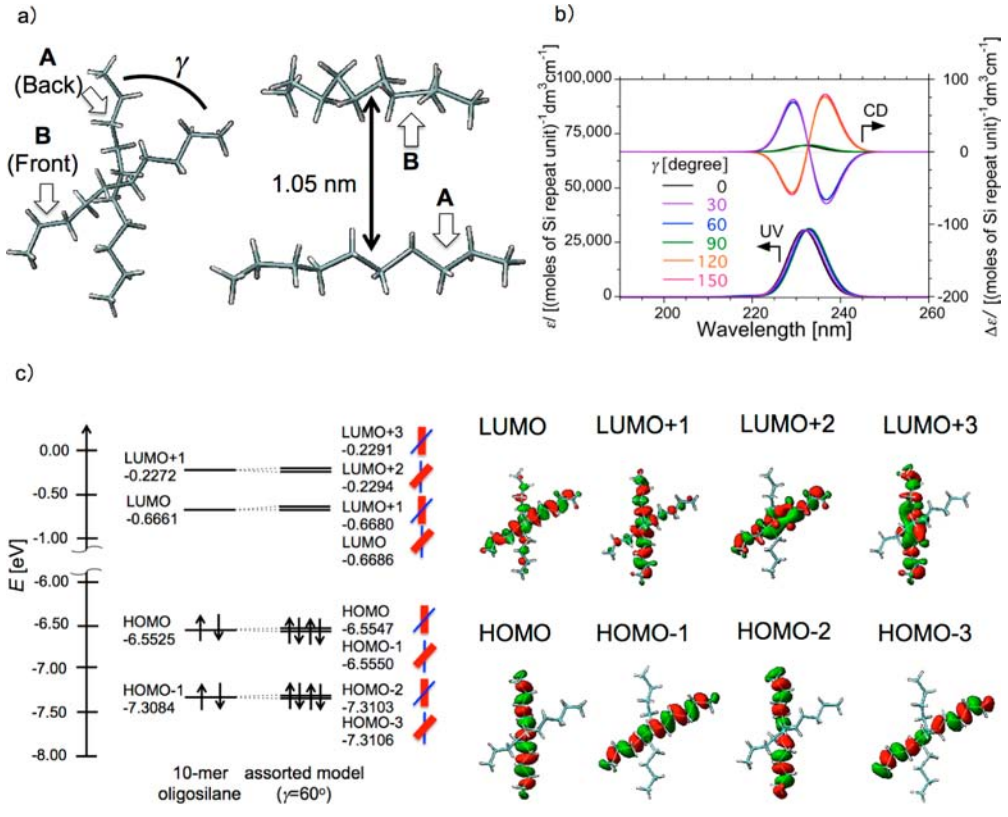

Figure 5. Selected results of Gaussian 03 calculations (TD-DFT, B3LYP/6-31G(d) basis set, inset is interchain spacing) using *P*-7_3 H−$(SiH_2)_{10}$−H (10-mer) with hydrogen termini. (a) Spatial arrangement of two 10-mers. The relative arrangement of molecules is set to the same as in Figure 4c. (b) Simulated CD (upper spectrum) and UV spectra (lower spectrum) as a function of γ. Bandwidth of the spectra were set to 0.1 eV. (c) Schematic molecular orbital (MO) diagrams of the single 10-mer and two 10-mers (γ = 60°). Crossing bold red and thin blue lines (drawn on the right side of HOMO and LUMO notation in the energy diagram) represent localized and nonlocalized electrons for the pairs of interacting model polymers.

contact with the poor solvent. Considering these three elements, the 2D-model, solvophobic effects, and aggregates of more than two molecules, it is reasonable to assume a twisted pasta-like form. These experimental realities could

dx.doi.org/10.1021/ja405570q | J. Am. Chem. Soc. 2013, 135, 13073−13079

account for any discrepancy between experimental results and model predictions, and justify discussing real, many molecule, aggregates as an extension of the two-component aggregate. The maintenance of the CD sign regardless of the toluene/methanol cosolvent ratio in **1** and **3**−**5** also supports the extension of the dimer model to aggregates with more than two components.

The combination of the cholesteric hard-core model and the exciton chirality method thus qualitatively provides a possible explanation of the observed side chain-dependent chiroptical inversion between **1** and **3**−**5** aggregates.

This consideration further led us to the idea that the solvent-dependent chiroptical inversion observed for **2** arises due to the differing solvation effects on the polymer side chains, i.e. side chain shrinking or stretching. When the volume ratio of toluene (lower polarity, good solvent) is relatively high, the alkyl side chain is well solvated and stretches away from the polymer chain (i.e., the d value is relatively large, leading to a negative bisignate Cotton effect). However, as the methanol (higher polarity, poor solvent) ratio increases, a large difference in polarity between solute polymer and cosolvent results in poor solvation of the nonpolar alkyl side chains, leading to contraction of the side chains toward the polymer chain (i.e., the d value becomes relatively small, leading to a positive bisignate Cotton effect).

Although the discussion above affords a plausible explanation for the two different kinds of chiroptical inversion effects, further analysis was required for discussion of (i) CD strength and (ii) highest occupied molecular orbital (HOMO) and lowest unoccupied molecular orbital (LUMO) states of pairs of interacting model polymers. To ascertain these points, TD-DFT (B3LYP/6-31G(d)) energy calculations using Gaussian 03[58] were carried out.

The calculated CD spectrum of a single molecule of H−$(SiH_2)_{10}$−H (dihedral angle $\theta = 150°$) showed a positive single-signed Cotton effect at 233 nm with $g_{CD} = 2.9 \times 10^{-4}$. The shorter wavelength of λ_{max} compared with the experimental value is likely to be due to reduced electronic delocalization stemming from the shorter main chain length.[24]

To obtain the exciton couplet spectra, several hypothetical models, each consisting of two 10-mers, were generated in GaussView 4.1. The γ (angular offset) values of the interacting models were set to 0°, 30°, 60°, 90°, 120°, and 150° setting the shortest interchain distance between the axes of molecules as 1.05 nm (Figure 5a) which is the distance between two 12-mers of **3** estimated from a single 12-mer model optimized by PM3 calculation.

The calculated CD for the models with γ = 30° and 60° showed negative bisignate signals, while for models with γ = 120° and 150°, positive signs were apparent, agreeing well with the exciton chirality method (Figure 5b).

The absolute magnitude of g_{CD} (the first Cotton band) at γ = 30°, 60°, 120°, and 150° was of the order of 3.0×10^{-3} to 4.4×10^{-3} and indeed enhanced by ca. 10−15 times compared to that of the isolated P-7_3 helical 10-mer. This calculation confirms the previously noted assumption that the signs and magnitudes of the Cotton effects in the aggregates predominantly arise from the exciton couplet effect rather than the intrinsic CD of the polysilane alone.

It is noted that when γ is 0° and 90°, the calculated g_{CD} values are 2.8×10^{-4} and 3.0×10^{-4}, respectively. These values are nearly equal to the g_{CD} value of the individual decamer model ($g_{CD} = 2.9 \times 10^{-4}$). This can be explained by applying the exciton chirality method to the interacting model cases.[60]

The MO diagrams of single 10-mer and two interacting 10-mer models are shown in Figure 4c. It should be noted that the number of nodes does not differ between the two splitting states. When the arrangement is chiral (γ = 30°, 60°, 120°, and 150°), electrons are mainly localized within both helices. In the case of γ = 60°, from the lower energy state (HOMO−3) to the higher energy state (LUMO+3), this localization appeared alternately in the upper and lower polymer molecules, which was not always the case for chiral arrangements (see HOMO, HOMO−1, HOMO−2, and HOMO−3 in SI, Figure S27).

Surprisingly, the excited states with the largest and second largest rotational strengths (excited states 1 and 2) were an admixture of intramolecular (major) and intermolecular transitions (minor). For the case of the model at γ = 60°, excited state 1 is composed of HOMO−1→LUMO, HOMO−1→LUMO+1, HOMO→LUMO, HOMO→LUMO+1, and their contributions were 34.7%, 10.7%, 11.0%, and 35.5%, respectively (Figure S18). Similar features were obtained for excited state 2 and the other pairs of interacting model polymer at γ = 30°, 60°, 120°, and 150°. This suggests the existence of partial charge transfer character in these models, though it is not a major factor.

Using our simple model, the present knowledge and understanding of aggregation-induced change in chiroptical properties should be applicable to other aggregate systems such as inorganic lanthanide complexes,[61] organic molecules,[62] synthetic macromolecules,[63] and crystals[64] in the future.

3. CONCLUSION

Side chain length-dependent (**1** and **3**−**5**) and cosolvent-dependent (**2**) CD inversions were realized by using a family of dialkylpolysilanes. The length of their side chains, which determines the helical diameter, appears to be the driving force responsible for the chiroptical inversion. The critical side chain length in the dialkylpolysilanes was that afforded by the *n*-propyl group. To explain these chiroptical inversion effects, we combined the cholesteric hard-core model and exciton chirality method, deriving, for the first time, a direct correlation between p/d ratio and the sign of the Cotton effect. The predicted signs agreed well with the results of side chain length-dependent chiroptical inversions in our dialkylpolysilane aggregation experiments. The solvent-dependent chiroptical inversion in **2** was considered to arise from solvent-dependent solvation effects on side chain extension. The relationship between the proposed higher order structures and chiroptical properties was further supported by Gaussian 03 calculations.

■ ASSOCIATED CONTENT

Supporting Information

Characterization data for the monomers and polymers, data of membrane filtration experiments, and details of the Gaussian 03 calculation. This material is available free of charge via the Internet at http://pubs.acs.org.

■ AUTHOR INFORMATION

Corresponding Author

fujikim@ms.naist.jp; koe@icu.ac.jp.

Notes

The authors declare no competing financial interest.

■ ACKNOWLEDGMENTS

We thank Profs. Hiroshi Daimon, Hironari Kamikubo, Shinji Koh, Aishi Yamamoto, Takahiro Sato, Kenya Kubo, Wang Jae Chun, Junji Kobayashi and Dr. Hidenori Ashima for inspiring discussions. We also thank Fumio Asanoma for assisting with NMR measurements. The work was supported by a Grant-in-Aid for Scientific Research (22350052) from JSPS and the Sekisui Chemical Grant Program for Research on Manufacturing Based on Learning from Nature (NAIST) and by MEXT: Supported Program for the Strategic Research Foundation at Private Universities 2008−2012 No. S0801012 (ICU). N.S. is grateful for the award of a JSPS research fellowship for young scientists.

■ REFERENCES

(1) Pauling, L.; Corey, R. B.; Branson, H. R. *Proc. Natl. Acad. Sci. U.S.A.* **1951**, *37*, 205−211.
(2) Watson, J. D.; Crick, F. H. *Nature* **1953**, *171*, 737−738.
(3) van Beijnen, A. J. M.; Nolte, R. J. M.; Zwikker, J. W.; Drenth, W. *J. Mol. Catal.* **1978**, *4*, 427−432.
(4) Rowan, A. E.; Nolte, R. J. M. *Angew. Chem., Int. Ed.* **1998**, *37*, 63−68.
(5) Okamoto, Y.; Suzuki, K.; Ohta, K.; Hatada, K.; Yuki, H. *J. Am. Chem. Soc.* **1979**, *101*, 4763−4765.
(6) Green, M. M.; Peterson, N. C.; Sato, T.; Teramoto, A.; Cook, R.; Lifson, S. *Science* **1995**, *268*, 1860−1866.
(7) Yashima, E.; Maeda, Y.; Matsushima, T.; Okamato, Y. *Chirality* **1997**, *9*, 593−600.
(8) Inouye, M.; Waki, M.; Abe, H. *J. Am. Chem. Soc.* **2004**, *126*, 2022−2027.
(9) Schlitzer, D. S.; Novak, B. M. *J. Am. Chem. Soc.* **1998**, *120*, 2196−2197.
(10) Katagiri, H.; Miyagawa, T.; Furusho, Y.; Yashima, E. *Angew. Chem., Int. Ed.* **2006**, *45*, 1741−1744.
(11) Lehn, J. M. *Proc. Natl. Acad. Sci. U.S.A.* **2002**, *99*, 4763−4768.
(12) Lehn, J. M.; Rigault, A.; Siegel, J.; Harrowfield, J.; Chevrier, B.; Moras, D. *Proc. Natl. Acad. Sci. U.S.A.* **1987**, *84*, 2565−2569.
(13) Piguet, C.; Bernardinelli, G.; Hopfgartner, G. *Chem. Rev.* **1997**, *97*, 2005−2062.
(14) Prince, R. B.; Barnes, S. A.; Moore, J. S. *J. Am. Chem. Soc.* **2000**, *122*, 2758−2762.
(15) Yan, N.; He, G.; Zhang, H.; Ding, L.; Fang, Y. *Langmuir* **2010**, *26*, 5909−5917.
(16) Feringa, B. L.; van Delden, R. A.; Koumura, N.; Geertsema, E. M. *Chem. Rev.* **2000**, *100*, 1789−1816.
(17) Langeveld-Voss, B. M. W.; Christiaans, M. P. T.; Janssen, R. A. J.; Meijer, E. W. *Macromolecules* **1998**, *31*, 6702−6704.
(18) Palmans, A. R. A.; Meijer, E. W. *Angew. Chem., Int. Ed.* **2007**, *46*, 8948−8968.
(19) Babudri, F.; Farinola, G. M.; Naso, F.; Ragni, R. *Chem. Commun.* **2007**, 1003−1022.
(20) Barnes, M. D.; Baghar, M. *J. Polym. Sci., Polym. Phys.* **2012**, *50*, 1121−1129.
(21) Roncali, J. *Chem. Rev.* **1992**, *92*, 711−738.
(22) Scherf, U.; List, E. J. W. *Adv. Mater.* **2002**, *14*, 477−487.
(23) Becker, S.; Ego, C.; Grimsdale, A. C.; List, E. J. W.; Marsitzky, D.; Pogantsch, A.; Setayesh, S.; Leising, G.; Müllen, K. *Synth. Met.* **2002**, *125*, 73−80.
(24) Miller, R. D.; Michl, J. *Chem. Rev.* **1989**, *89*, 1359−1410.
(25) Fujiki, M. *J. Am. Chem. Soc.* **1994**, *116*, 11976−11981.
(26) West, R. *J. Organomet. Chem.* **1986**, *300*, 327−346.
(27) Dellaportas, P.; Jones, R. G.; Holder, S. J. *Macromol. Rapid Commun.* **2002**, *23*, 99−103.
(28) Ohira, A.; Okoshi, K.; Fujiki, M.; Kunitake, M.; Naito, M.; Hagihara, T. *Adv. Mater.* **2004**, *16*, 1645−1650.
(29) Peng, W.; Motonaga, M.; Koe, J. R. *J. Am. Chem. Soc.* **2004**, *126*, 13822−13826.
(30) Goto, H.; Okamoto, Y.; Yashima, E. *Macromolecules* **2002**, *35*, 4590−4601.
(31) Satrijo, A.; Swager, T. M. *Macromolecules* **2005**, *38*, 4054−4057.
(32) Satrijo, A.; Meskers, S. C. J.; Swager, T. M. *J. Am. Chem. Soc.* **2006**, *128*, 9030−9031.
(33) Wu, L.; Sato, T. *Kobunshi Ronbunshu* **2006**, *63*, 505−511.
(34) Nakano, Y.; Fujiki, M. *Macromolecules* **2011**, *44*, 7511−7519.
(35) Pijper, D.; Jongejan, M. G. M.; Meetsma, A.; Feringa, B. L. *J. Am. Chem. Soc.* **2008**, *130*, 4541−4552.
(36) Tabei, J.; Nomura, R.; Shiotsuki, M.; Sanda, F.; Masuda, T. *Macromol. Chem. Phys.* **2005**, *206*, 323−332.
(37) Fujiki, M.; Koe, J. R.; Terao, K.; Sato, T.; Teramoto, A.; Watanabe, J. *Polym. J.* **2003**, *35*, 297−344.
(38) Rizzo, P.; Beltrani, M.; Guerra, G. *Chirality* **2010**, *22*, E67−E73.
(39) Kyotani, H.; Shimomura, M.; Miyazaki, M.; Ueno, K. *Polymer* **1995**, *36*, 915−919.
(40) Takeda, K.; Teramae, H.; Matsumoto, N. *J. Am. Chem. Soc.* **1986**, *108*, 8186−8190.
(41) Takeda, K.; Fujino, M.; Seki, K.; Inokuchi, H. *Phys. Rev. B* **1987**, *36*, 8129−8137.
(42) Straley, J. P. *Phys. Rev. A* **1976**, *14*, 1835−1841.
(43) Harris, A. B.; Kamien, R. D.; Lubensky, T. C. *Rev. Mod. Phys.* **1999**, *71*, 1745−1757.
(44) Gottarelli, G.; Spada, G. P. In *Circular Dichroism*, 2nd ed.; Berova, N., Nakanishi, K., Woody, R., Eds.; Wiley-VCH: New York, NY, 2000; Chapter 19.
(45) Harada, N.; Nakanishi, K. *Acc. Chem. Res.* **1972**, *5*, 257−263.
(46) Harada, N.; Chen, S. M. L.; Nakanishi, K. *J. Am. Chem. Soc.* **1975**, *97*, 5345−5352.
(47) Berova, N.; Nakanishi, K. In *Circular Dichroism*, 2nd ed.; Berova, N., Nakanishi, K., Woody, R., Eds.; Wiley-VCH: New York, NY, 2000; Chapter 12.
(48) Berova, N.; Bari, L. D.; Pescitelli, G. *Chem. Soc. Rev.* **2007**, *36*, 914−931.
(49) Okoshi, K.; Kamee, H.; Suzaki, G.; Tokita, M.; Fujiki, M.; Watanabe, J. *Macromolecules* **2002**, *35*, 4556−4559.
(50) Fujiki, M. *Appl. Phys. Lett.* **1994**, *65*, 3251−3253.
(51) Fujiki, M. *Symmetry* **2010**, *2*, 1625−1652.
(52) Tsuji, H.; Fukazawa, A.; Yamaguchi, S.; Toshimitsu, A.; Tamao, K. *Organometallics* **2004**, *23*, 3375−3377.
(53) Tsuji, H.; Terada, M.; Toshimitsu, A.; Tamao, K. *J. Am. Chem. Soc.* **2003**, *125*, 7486−7487.
(54) Tsuji, H.; Michl, J.; Tamao, K. *J. Organomet. Chem.* **2003**, *685*, 9−14.
(55) Kasha, M. *Radiat. Res.* **1963**, *20*, 55−71.
(56) Kasha, M.; Rawls, H. R.; El-Bayoumi, M. A. *Pure Appl. Chem.* **1965**, *11*, 371−392.
(57) When an individual polymer chain is regarded as a long rigid cylinder, *J*-aggregates reduce the solvent-exposed area by only the small top and bottom surfaces of the two ends of two polymer molecules, while *H*-aggregates result in a much larger surface reduction due to exclusion of solvent from the curved side surfaces of the chains.
(58) Frisch, M. J.; Trucks, G. W.; Schlegel, H. B.; Scuseria, G. E.; Robb, M. A.; Cheeseman, J. R.; Montgomery, J. A., Jr.; Vreven, T.; Kudin, K. N.; Burant, J. C.; Millam, J. M.; Iyengar, S. S.; Tomasi, J.; Barone, V.; Mennucci, B.; Cossi, M.; Scalmani, G.; Rega, N.; Petersson, G. A.; Nakatsuji, H.; Hada, M.; Ehara, M.; Toyota, K.; Fukuda, R.; Hasegawa, J.; Ishida, M.; Nakajima, T.; Honda, Y.; Kitao, O.; Nakai, H.; Klene, M.; Li, X.; Knox, J. E.; Hratchian, H. P.; Cross, J. B.; Bakken, V.; Adamo, C.; Jaramillo, J.; Gomperts, R.; Stratmann, R. E.; Yazyev, O.; Austin, A. J.; Cammi, R.; Pomelli, C.; Ochterski, J. W.; Ayala, P. Y.; Morokuma, K.; Voth, G. A.; Salvador, P.; Dannenberg, J. J.; Zakrzewski, V. G.; Dapprich, S.; Daniels, A. D.; Strain, M. C.; Farkas, O.; Malick, D. K.; Rabuck, A. D.; Raghavachari, K.; Foresman, J. B.; Ortiz, J. V.; Cui, Q.; Baboul, A. G.; Clifford, S.; Cioslowski, J.; Stefanov, B. B.; Liu, G.; Liashenko, A.; Piskorz, P.; Komaromi, I.; Martin, R. L.; Fox, D. J.; Keith, T.; Al-Laham, M. A.; Peng, C. Y.; Nanayakkara, A.; Challacombe, M.; Gill, P. M. W.; Johnson, B.; Chen,

W.; Wong, M. W.; Gonzalez, C.; Pople, J. A.; *Gaussian 03*, Revision E.01; Gaussian, Inc.: Wallingford, CT, 2004.

(59) We assume the discrepancy in the critical value between the cholesteric hard-core model and the experiment is due to neglect of other contact modules. The cholesteric hard core approach describes wing-and-core contact, for which $p/d \ll \pi$. However, in the case of a double helix, there should be wing−wing contact and/or core−core contact. Such a contact module is understandable for $p/d \gg \pi$ in a reference.[42] Despite neglect of the other contact modes, the model describes $p/d \ll \pi$ and the tendency of p/d well. At $p/d \ll \pi$, neither wing−wing nor core-and-core contact will be stable. This is because for wing−wing contact, the packing between the helices is bad (i.e., distance between two helices is great). For core-and-core, contact is impossible because the pitch is too short, and core-and-core contact would be prevented by the wings. Thus the cholesteric hard core model is appropriate to describe the situation $p/d \ll \pi$ and the tendency but not appropriate for predicting the critical value.

(60) According to the exciton chirality method,[48] $\Delta\varepsilon$ can be expressed by

$$\Delta\varepsilon \propto \pm\Gamma(\lambda, \lambda_0)R_{12}V_{12} \tag{2}$$

where Γ accounts for dispersive couplet shape, V_{12} for Davydov potential, R_{12} for rotational strength of the exciton coupling between two electric transition dipole moment, λ_0 for transition wavelength, and λ for variable wavelength. In general, the V_{12} and R_{12} can be expressed as

$$R_{12} \propto \vec{r}_{12}\cdot(\vec{\mu}_1 \times \vec{\mu}_2) = \mu_1\mu_2 r_{12}[\vec{e}_{12}\cdot(\vec{e}_1 \times \vec{e}_2)] \tag{3}$$

$$V_{12} = \frac{\mu_1\mu_2}{r_{12}^3}[\vec{e}_1\cdot\vec{e}_2 - 3(\vec{e}_1\cdot\vec{e}_{12})(\vec{e}_2\cdot\vec{e}_{12})] \tag{4}$$

where vectors μ_1 and μ_2 are electric transition dipole moment of chromophores 1 and 2, vector r_{12} indicates a distance from the center of μ_1 to that of μ_2. Vectors e_1, e_2, and e_{12} are unit vectors of vector μ_1, μ_2, and r_{12}, respectively. For the case of interacting models (γ = 0°, 30°, 60°, 90°, 120°, and 150°), it can be assumed that e_1 and e_{12} as well as e_2 and e_{12} are nearly orthogonal to each other, thus $e_1\cdot e_{12}$ becomes 0, as well as $e_2\cdot e_{12}$ becomes 0. Therefore V_{12} can be approximated as follows.

$$V_{12} \approx \frac{\mu_1\mu_2}{r_{12}^3}[\vec{e}_1\cdot\vec{e}_2] \tag{5}$$

Therefore, $\Delta\varepsilon$ can be written as

$$\Delta\varepsilon \propto \pm\Gamma(\lambda, \lambda_0)\frac{\mu_1^2\mu_2^2}{r_{12}^2}[\vec{e}_{12}\cdot(\vec{e}_1 \times \vec{e}_2)][(\vec{e}_1\cdot\vec{e}_2)] \tag{6}$$

Equation 6 suggests that at γ = 0°, $\boldsymbol{R}_{12}$ becomes 0 since its component $e_1 \times e_2$ becomes 0. On the other hand, at γ = 90°, $\boldsymbol{V}_{12}$ becomes 0 because the dot product of the two transition dipole moments $e_1\cdot e_2$ becomes 0. Thus the electric transition coupling disappears and shows only the optical activity of the two individual decamer chains at γ = 0° and 90°.

(61) Kitchen, J. A.; Barry, D. E.; Mercs, L.; Albrecht, M.; Peacock, R. D.; Gunnlaugsson, T. *Angew. Chem., Int. Ed.* **2012**, *51*, 704−708.

(62) Hong, Y.; Lam, J. W. Y.; Tang, B. Z. *Chem. Commun.* **2009**, 4332−4353.

(63) Hayasaka, H.; Miyashita, T.; Tamura, K.; Akagi, K. *Adv. Funct. Mater.* **2010**, *20*, 1243−1250.

(64) Phillips, K. E. S.; Katz, T. J.; Jockusch, S.; Lovinger, A. J.; Turro, N. J. *J. Am. Chem. Soc.* **2001**, *123*, 11899−11907.